HHS Public Access

Author manuscript

Eur J Neurol. Author manuscript; available in PMC 2017 February 14.

Published in final edited form as:

Eur J Neurol. 2016 October ; 23(10): 1517–1527. doi:10.1111/ene.13067.

Cortical sensorimotor alterations classify clinical phenotype and putative genotype of spasmodic dysphonia

Giovanni Battistella[1], **Stefan Fuertinger**[1], **Lazar Fleysher**[2], **Laurie J. Ozelius**[3], and **Kristina Simonyan**[1,4,*]

[1]Department of Neurology, Icahn School of Medicine at Mount Sinai, New York, NY, USA

[2]Department of Radiology, Icahn School of Medicine at Mount Sinai, New York, NY, USA

[3]Department of Neurology, Massachusetts General Hospital, Charlestown, MA USA

[4]Department of Otolaryngology, Icahn School of Medicine at Mount Sinai, New York, NY, USA

Abstract

Background—Spasmodic dysphonia (SD), or laryngeal dystonia, is a task-specific isolated focal dystonia of unknown causes and pathophysiology. Although functional and structural abnormalities have been described in this disorder, the influence of its different clinical phenotypes and genotypes remains scant, making it difficult to explain SD pathophysiology and to identify potential biomarkers.

Methods—We used a combination of independent component analysis and linear discriminant analysis of resting-state functional MRI data to investigate brain organization in different SD phenotypes (abductor vs. adductor type) and putative genotypes (familial vs. sporadic cases) and to characterize neural markers for genotype/phenotype categorization.

Results—We found abnormal functional connectivity within sensorimotor and frontoparietal networks in SD patients compared to healthy individuals as well as phenotype- and genotype-distinct alterations of these networks, involving primary somatosensory, premotor and parietal cortices. The linear discriminant analysis achieved 71% accuracy classifying SD and healthy individuals using connectivity measures in the left inferior parietal and sensorimotor cortex. When categorizing between different forms of SD, the combination of measures from left inferior parietal, premotor and right sensorimotor cortices achieved 81% discriminatory power between familial and sporadic SD cases, whereas the combination of measures from the right superior parietal, primary somatosensory and premotor cortices led to 71% accuracy in the classification of adductor and abductor SD forms.

[*]*Corresponding author:* Kristina Simonyan, MD, PhD, Department of Neurology, One Gustave L. Levy Place, Box 1137, Icahn School of Medicine at Mount Sinai, New York, NY 10029, Tel.: (212) 241-0656, Fax: (646) 537-8628, kristina.simonyan@mssm.edu.

Disclosure of conflict of interest: GB – none; SF - none; LF – none; LJO serves on the Scientific Advisory Boards of the Benign Essential Blepharospasm Research Foundation, National Spasmodic Dysphonia Association, National Tourette's Syndrome Association and Cure AHC; she receives royalties from Athena Diagnostics; KS serves on the Medical and Scientific Advisory Council of the Dystonia Medical Research Foundation.

Conclusions—Our findings present the first effort to identify and categorize isolated focal dystonia based on its brain functional connectivity profile, which may have a potential impact on the future development of biomarkers for this rare disorder.

Keywords

dystonia; resting-state networks; imaging marker

Introduction

Spasmodic dysphonia (SD), or laryngeal dystonia, is a task-specific focal dystonia affecting the laryngeal muscles predominantly during speaking but not during emotional vocalizations, such as laughing or crying. As with other forms of focal dystonia, the causes and pathophysiology of SD remain unclear, although its clinical symptoms are well defined [1, 2]. Existing literature reports the presence of structural and functional abnormalities in the primary sensorimotor and secondary somatosensory cortices, basal ganglia, thalamus, and cerebellum [3-10], which appear to constitute the dystonic brain network [11] and also contribute to the control of sensorimotor aspects of speech production [12]. In addition, striatal dopaminergic function is altered in SD, characterized by decreased availability of D_2/D_3 receptors and abnormal release of endogenous dopamine during symptomatic and asymptomatic tasks [13]. However, despite the considerable progress made in mapping brain alterations in SD, our understanding of the interplay between disorder etiology and pathophysiology remains very limited. Specifically, it is unknown whether any of these reported brain abnormalities may be considered as a neuroimaging marker(s) for SD prediction and diagnostic differentiation. This is partly due to the fact that the majority of studies focused on mapping brain alterations in the most common sporadic adductor form of SD, thus rendering difficult to employ classifier algorithms for disorder characterization and the assessment of a more complete pathophysiological picture of this disorder across its different phenotypes and genotypes.

In a large cohort of SD patients, we examined distinct patters of abnormal functional connectivity and predictive imaging markers of disorder categorization between adductor (ADSD) and abductor (ABSD) forms of SD as well as between sporadic and familial cases as representatives of potentially different genotypes. We used multivariate classification algorithm of linear discriminant analysis (LDA) using the measures of between-group differences in resting-state functional connectivity derived from an independent component analysis (ICA). Resting-state networks are based on the measure of intrinsic low frequency physiological fluctuations in the blood-oxygen-level-dependent (BOLD) signal and reflect the organization of both structural and task-related functional brain networks [14-16]. Patients with different forms of focal dystonia have been previously reported to exhibit altered resting-state connectivity [17-21]. Classification algorithms represent a powerful tool for identification of single traits or a combination of features that characterize and separate between two or more classes of objects or subjects. Algorithmic classifiers have been successfully applied in several neurodegenerative disorders using structural [22, 23] and functional MRI measures [24-26]. Machine learning and fMRI voxel-wise multivariate classification were implemented as powerful tools for decoding neural representations of

thoughts or physical objects at a particular time-point [27-29], with the LDA being validated in both normal [30-33] and disordered states [34-37].

Based on prior studies in SD [3-10], we hypothesized that SD as a disorder can be distinguished from a normal state based on significant alterations within the sensorimotor network, whereas different SD forms can be categorized based on additional and combined abnormalities within sensorimotor and fronto-parietal networks. Because SD is a task-specific disorder impairing a highly learned behavior, i.e., speech, we hypothesized that the predictive imaging markers for SD phenotype/genotype categorization would be found within cortical rather than subcortical regions.

Methods

Study Participants

We recruited 98 SD patients, who were grouped based on their clinical phenotype (ADSD and ABSD) and underlying putative genotype (sporadic and familial SD). Among these, 15 patients were excluded due to excessive motion artifacts and incidental neuroradiological findings. The final groups consisted of 60 sporadic SD (30 ABSD/30 ADSD) and 23 familial SD (18 ADSD/5 ABSD) as well as 30 age- and gender-matched healthy volunteers (see demographic details in Table 1).

All participants were monolingual, native English speakers, and had normal scores on the Mini-Mental State Examination. With the exception of one familial SD patient, all participants were right-handed as determined by the Edinburgh Handedness Inventory. None of participants had a past or present history of any neurological (other than SD), psychiatric or laryngeal disorders. Diagnosis of SD was confirmed based on fiberoptic nasolaryngoscopy. All patients were fully symptomatic and had abstained from botulinum toxin injections for at least three months prior to the study.

All participants provided written informed consent, which was approved by the Internal Review Board at the Icahn School of Medicine at Mount Sinai.

MRI acquisition protocol

Whole-brain images were acquired on a Phillips 3T scanner equipped with an 8-channel head-coil. Resting-state fMRI data were obtained using a single-shot echo-planar imaging (EPI) gradient echo sequence, repetition time (TR) = 2000 ms, echo time (TE) = 30ms, flip angle = 90, field of view (FOV) = 240 mm, voxel size = 3x3mm with 33 slices of 3.5 mm. A total of 150 volumes were acquired during a 5-min scan. Participants were instructed to keep their eyes closed without falling asleep or thinking of anything in particular during scanning. A sagittal T1-weighted gradient-echo sequence (MPRAGE: 172 contiguous slice, 1 mm^3 voxel, TR = 7.5 ms, TE = 3.5ms, FOV = 210 mm) was acquired for brain segmentation and functional image registration. Head movements during scanning were minimized by cushioning the participant's head in the coil; all subjects were monitored for any movements while in the scanner.

Data analysis

Preprocessing—Resting-state fMRI data were preprocessed using FSL and AFNI software. Following the removal of the first 4 volumes due to possible T1 stabilization effects, intra-session acquisitions were re-aligned to the fifth scan using a six-parameter rigid-body transformation and high-pass filtered with a cutoff frequency of 0.01 Hz (Gaussian-weighted least squares straight line fitting). Resultant images were then co-registered to the respective anatomical acquisition and normalized to the AFNI standard Talairach-Tournoux brain using a 12-parameter affine transformation with the follow-up optimization of normalization using a non-linear algorithm in AFNI software. To control for possible motion and physiological noise effects, 4D time series in each subject were regressed using eight parameters, including white matter (WM) and cerebrospinal fluid (CSF) mean signal and six motion parameters calculated during realignment. WM and CSF covariates were extracted by automatically segmenting the MPRAGE into the GM, WM and CSF using the unified segmentation approach [38] in SPM8 software. WM and CSF maps were thresholded at 90% of tissue probability and applied to each time series. All voxels in the masks were then averaged across all time series to extract nuisance regressors. Final images were smoothed using a 5-mm Gaussian kernel full-width at half-maximum (FWHM) and mean-based intensity normalized as an input for group ICA analysis.

Feature selection—Multivariate classification methods consisted of three main stages: (1) feature extraction; (2) dimensionality reduction, and (3) feature-based classification with cross-validation [39]. Feature selection was used to reduce the number of features and remove irrelevant and redundant data, thus improving classification performance. As an input to the LDA, we used the features extracted from a multivariate ICA. For this, pre-processed time series in all subjects were concatenated and decomposed into spatially independent components using a temporal concatenation approach [40] implemented in the MELODIC tool (Multivariate Exploratory Linear Optimized Decomposition into Independent Components) of FSL software. All obtained components were visually examined, and those that were spatially similar to previously identified networks [40, 41] and had relevance to dystonia pathophysiology [17, 19, 20, 42, 43] were extracted for further between-group analysis using dual regression [31, 44]. Voxel-based inferential statistics were computed using the individual Z-value maps of the dual regression. One-way analysis of variance (ANOVA) was used to assess the overall group differences between 30 healthy controls and 32 SD patients, including 16 sporadic and 16 familial cases with a balanced representation of patients with ADSD and ABSD. To examine the effects of SD genotype and phenotype on resting-state connectivity profiles, we compared (1) 30 sporadic SD to 23 familial SD and (2) 35 ADSD (30 sporadic and 5 familial cases) to 35 ABSD (30 sporadic and 5 familial cases), respectively. Statistical thresholds were set at a corrected family-wise error (FWE) $p \leq 0.01$ to account for multiple comparisons. Significant clusters derived from between-group analyses were used in the subsequent classification analyses to identify the most informative brain region or the combination of regions that maximized the differentiation of SD patients from healthy controls; ADSD from ABSD patients, and sporadic from familial SD cases.

Linear discriminant analysis (LDA)—The mean signal of each significant cluster in between-group ICA comparisons was used as a feature of the LDA. To reduce the initial number of extracted features, we used a variable ranking procedure and a feed-forward selection procedure [39]. The first step ranked the features using the absolute value of the standardized *U*-statistic of a two-sample Wilcoxon test. This allowed the ranking of variables by optimizing the covariance matrix for subsequent feature classification based on the minimum number of significant features. The ordered variables were included as predictors in the LDA, starting from the highest rank and subsequently adding more features in the order of decreasing rank. Variable selection was stopped after the best discrimination power was achieved. The latter was defined as the percentage of correctly classified samples in a leave-1-out cross-validation procedure, that is, an iterative removal of one subject from the dataset, construction of the predictor for the remaining data, and classification of the removed subject [39].

Results

The initial ICA analysis identified both shared and distinct patterns of abnormal resting-state functional connectivity within the sensorimotor (SMN), frontoparietal (FPN) but not default-mode network across different phenotypes and genotypes of SD at an FWE-corrected $p \leq 0.01$.

The SMN is generally composed of functionally connected regions in the prefrontal cortex, premotor cortex and primary sensorimotor cortices as well as inferior and superior parietal cortices [16, 45] (Fig. 1A). Compared to healthy controls, all SD patients showed decreased functional connectivity in the left sensorimotor cortex, inferior parietal cortex, putamen, right parietal operculum, and bilateral supplementary motor area (SMA) (Fig. 1B-I, Table 2). A direct comparison between sporadic and familial patients showed specific alterations of functional connectivity in the left sensorimotor cortex, right somatosensory cortex, SMA and insula as a potential influence of SD genotype (Fig. 1B-II, Table 2). A direct comparison between ADSD and ABSD groups found phenotype-specific differences in SMN connectivity in the right superior parietal cortex (Fig. 1B-III, Table 2).

The FPN is typically a left-lateralized spatial component that comprises extended regions of the parietal, inferior and middle frontal cortices, strongly corresponding to functional brain activity during cognitive and language processing [16, 45] (Fig. 2A). Compared to healthy controls, all SD patients showed increased functional connectivity in the left inferior parietal cortex (Fig. 2B-I, Table 2), with familial SD patients exhibiting further abnormalities in this region compared to sporadic SD (Fig. 2B-II, Table 2). No significant clusters of distinctly abnormal FPN connectivity were identified in the direct comparison between ADSD and ABSD patients.

The default mode network, one of the most widely studied resting-state networks, includes medial parietal regions (precuneus and posterior cingulate cortex) and ventromedial frontal cortex and is thought to characterize basic resting neural activity [16, 45]. We did not find any significant differences in default mode network either between healthy controls and SD patients or between the different SD subgroups.

Linear discriminant analysis

SD patients vs. healthy controls—Based on data from the ICA analysis, the identified six clusters of functional connectivity alterations within the SMN and FPN (Table 2) were sorted by explanatory power for classification between disordered and normal states. The obtained rank (in decreasing order) included the left inferior parietal cortex, sensorimotor cortex, SMA, putamen, parietal operculum, and right superior temporal gyrus. Using the single, top-ranked cluster within the left inferior parietal cortex as a feature in the LDA, the accuracy of classification between SD patients and healthy controls was 50% with 17 out of 32 patients and 14 out 30 controls being misclassified (Table 3). However, classification performance considerably improved when the LDA was based on the combination of the left inferior parietal and primary sensorimotor cortices, leading to a classification accuracy of 71%, with 9 out of 32 SD patients and 9 out of 30 controls remaining misclassified (Fig. 3-I). Classification power did not improve from adding a third or more features (accuracy rate ≤ 64.5%).

Sporadic vs. familial SD—Sorting the most explanatory features for SD putative genotype categorization between patients with sporadic and familial SD, resulted in the following ranking of the four clusters of functional connectivity alterations (Table 2): the left inferior parietal cortex, right somatosensory cortex, left premotor cortex, and right SMA (in decreasing order). Using only the highest ranked feature in the LDA, i.e., the left inferior parietal cortex, the accuracy of classification between sporadic and familial SD patients was 68%, with 8 out of 23 familial SD and 9 out of 30 sporadic SD being misclassified. The best overall classification power of 81% accuracy between these two patient groups was obtained with the combination of left inferior parietal, premotor and right somatosensory cortices, with 3 out of 23 familial SD and 7 out of 30 sporadic SD being misclassified (Fig. 3-II, Table 3). The overall classification power did not improve by considering other combinations of the four brain regions (accuracy rate ≤ 81%).

ADSD vs. ABSD—We identified only one region of significant functional alteration between ADSD and ABSD patients, which was located in the right superior parietal cortex and yielded 65% accuracy (13 out of 35 ADSD and 11 out of 35 ABSD misclassified) of the LDA classifier when distinguishing between the two clinical phenotypes of SD (Table 3). Because this accuracy rate was suboptimal, we lowered our statistical threshold from an FWE-corrected $p \leq 0.01$ to an FWE-corrected $p \leq 0.05$ in order to identify additional regions of abnormalities between these groups for a more comprehensive discriminative analysis. This strategy led to identification of further abnormalities in functional connectivity in the right primary somatosensory cortex and right premotor cortex between ADSD and ABSD patients. The classification power between ADSD and ABSD patients based on the combination of the right superior parietal, primary somatosensory and premotor cortices increased to 71%, with 12 out of 35 ADSD and 8 out of 35 ABSD being misclassified (Fig. 3-III).

Discussion

Our study demonstrated that SD patients exhibited functional connectivity alterations within the sensorimotor and frontoparietal networks, which varied in their extent between different clinical phenotypes (ADSD vs. ABSD) and which might have been influenced by the involvement of different genetic factors in familial and sporadic cases. We further showed that abnormalities in the sensorimotor and parietal regions may serve as imaging markers for identification of SD as a disorder and its further classification into different subtypes (ADSD vs. ABSD; sporadic vs. familial SD). Specifically, combined alterations in the left inferior parietal and sensorimotor cortices permitted a reliable classification of SD patients and healthy controls. A combination of abnormal functional connectivity measures in the right somatosensory cortex and left inferior parietal and premotor cortices showed high accuracy in distinguishing between sporadic and familial SD cases, whereas right-sided alterations in the superior parietal, primary somatosensory and premotor cortices defined distinct ADSD and ABSD phenotypes. As such, our study not only mapped functional network alterations in this disorder, but also used neuroimaging data to disambiguate SD from a normal state and differentiate the disorder based on its clinical and genetic heterogeneity, pointing to possible mechanistic aspects of SD pathophysiology.

Identification of SD as a disorder

Our overall findings show greater impairment of the cortical network in SD, with major alterations identified in resting-state networks involved in the control of sensorimotor processing and motor planning (sensorimotor network) as well as multisensory integration and speech/language (frontoparietal network) [16, 40]. Although the basal ganglia have been considered as a key region in the pathophysiology of dystonia [46-48] and we did observe significantly reduced functional connectivity of the left putamen in this study, the greater involvement of cortical network abnormalities in SD pathophysiology and their combined accuracy in classifying this disorder may not be surprising. The extent of cortical network alterations may be explained by the fact that SD primarily affects speech production, which is a highly learned and skillful behavior, deeply relying on fine orchestration of multiple cortical networks [12, 49, 50]. Furthermore, the presence of predominantly left-sided network alterations may be reflected by the left-hemispheric dominance of speech controlling networks in right–handed individuals, which appears to be affected in SD patients. On the other hand, the left putamen, which we found to have decreased connectivity within the sensorimotor network, has been previously shown to exhibit reduced functional activity during symptomatic but not asymptomatic voice production [5], increased gray matter volume [6], and decreased D_2/D_3 receptor availability and endogenous dopamine release in SD patients [13]. While our present findings do not refute the notion that the putamen is involved in the pathophysiology of dystonia, it appears that functional alterations in this region may not provide sufficient discriminative information for accurate SD classification.

Contrary to some earlier studies in other forms of focal dystonia [19, 20, 42], we did not observe any significant alterations of the default-mode network in SD patients. This discrepancy might be due to SD-specific brain organization, which is likely characterized by

intrinsic networks controlling complex sensorimotor and executive tasks rather than the absence of specific goal-directed behaviors.

In comparison with healthy individuals, all SD patients showed significant decreases in functional connectivity of the left primary sensorimotor/premotor cortex, putamen, inferior parietal lobule, bilateral SMA, as well as right parietal operculum and primary auditory cortex. Using these significant network abnormalities for the identification of the disordered state, we found that the combination of alterations in the left sensorimotor cortex and inferior parietal lobule provide 71% accuracy in classifying SD and healthy individuals. Functional and structural MRI studies as well as the assessments of cortical excitability with transcranial magnetic stimulation (TMS) have previously reported alterations in sensorimotor regions in SD [3-6, 9, 51, 52] and other forms of dystonia [53, 54], pointing to their role in dystonia pathophysiology. Modulation of abnormal laryngeal and cortical sensorimotor activity following the treatment with botulinum toxin injections has also been hypothesized to be relevant to SD pathophysiology [3, 55], although the literature in this domain remains somewhat scant and inconsistent [3, 4]. Being well integrated in the sensorimotor interface [56-60], reduced activation of the parietal cortex in dystonic patients has been associated with impaired processing of sensory information and abnormal coupling between sensory input and motor output [42, 61] as well as abnormal proprioceptive input via cerebellar connections [62, 63]. Our current findings support a major role of the parietal cortex in the pathophysiology of dystonia in general and SD in particular and further highlight the importance of the left inferior parietal cortex (together with the left sensorimotor cortex) as a neuroimaging marker for SD discrimination from a normal state.

Identification of SD based on phenotype and genotype

Even though causative genes of SD have not yet been identified, cumulative evidence suggests that genetic susceptibility factors or dominantly inherited genes with reduced penetrance may be involved in SD genetic pathophysiology [64-66]. Our current findings of additional alterations of both sensorimotor and frontoparietal networks in familial vs. sporadic SD cases suggest a possible effect of these genetic risk factors (albeit unknown) on functional connectivity alterations in familial vs. sporadic SD cases. On the other hand, we found that the influence of SD phenotype was limited to distinct alterations within the sensorimotor network only, suggesting that dystonia phenotype may be provoked by differences in processing and execution of specific motor commands in ABSD vs. ADSD patients. Furthermore, strictly right-lateralized abnormalities between ABSD and ADSD patients may speak to possibly abnormal functional integration of both hemispheres in this disorder. Taken together, the presence of distinct alterations in functional connectivity between different forms of SD suggests the influence of phenotypic and genotypic characteristics on brain organization and sheds light on divergent, multifactorial pathophysiological pathways underlying distinct phenotype and genotype-specific relationships in this disorder.

In conclusion, we found that, among all regions with reduced connectivity, the parietal cortex was one of the strongest regions that reliably discriminated between different SD clinical phenotypes and putative genotypes. Its discriminatory power was aided by addition

of sensorimotor regions, which further underscores the parietal cortex as a possible imaging marker for identification and categorization of SD. As a fairly simple setup and a short acquisition time of resting-state fMRI datasets make its translation from a research methodology to clinical neuroradiology feasible, the results of our study provide a scientific foundation for further tests of more complex classification algorithms in larger patient cohorts with the ultimate goal to translate and implement the current findings in clinical practice as well as to help stratifying patients for future studies involving gene discovery and clinical trials.

Acknowledgments

We thank Estee Rubien-Thomas, BA, and Heather Alexander, BA, for patient recruitment and imaging data acquisition. This work was supported by R01DC01805 grant to KS from the National Institute on Deafness and Other Communication Disorders, National Institutes of Health.

References

[1]. Blitzer A. Spasmodic dysphonia and botulinum toxin: experience from the largest treatment series. Eur J Neurol. 2010; 17(Suppl 1):28–30. [PubMed: 20590805]

[2]. Brin MF, Blitzer A, Stewart C. Laryngeal dystonia (spasmodic dysphonia): observations of 901 patients and treatment with botulinum toxin. Adv Neurol. 1998; 78:237–252. [PubMed: 9750921]

[3]. Ali SO, Thomassen M, Schulz GM, et al. Alterations in CNS activity induced by botulinum toxin treatment in spasmodic dysphonia: an H215O PET study. Journal of speech, language, and hearing research : JSLHR. 2006; 49:1127–1146.

[4]. Haslinger B, Erhard P, Dresel C, Castrop F, Roettinger M, Ceballos-Baumann AO. "Silent event-related" fMRI reveals reduced sensorimotor activation in laryngeal dystonia. Neurology. 2005; 65:1562–1569. [PubMed: 16301482]

[5]. Simonyan K, Ludlow CL. Abnormal activation of the primary somatosensory cortex in spasmodic dysphonia: an fMRI study. Cereb Cortex. 2010; 20:2749–2759. [PubMed: 20194686]

[6]. Simonyan K, Ludlow CL. Abnormal structure-function relationship in spasmodic dysphonia. Cereb Cortex. 2012; 22:417–425. [PubMed: 21666131]

[7]. Simonyan K, Tovar-Moll F, Ostuni J, et al. Focal white matter changes in spasmodic dysphonia: a combined diffusion tensor imaging and neuropathological study. Brain. 2008; 131:447–459. [PubMed: 18083751]

[8]. Samargia S, Schmidt R, Kimberley TJ. Cortical Silent Period Reveals Differences Between Adductor Spasmodic Dysphonia and Muscle Tension Dysphonia. Neurorehabil Neural Repair. 2015

[9]. Suppa A, Marsili L, Giovannelli F, et al. Abnormal motor cortex excitability during linguistic tasks in adductor-type spasmodic dysphonia. Eur J Neurosci. 2015; 42:2051–2060. [PubMed: 26061279]

[10]. Kostic VS, Agosta F, Sarro L, et al. Brain structural changes in spasmodic dysphonia: A multimodal magnetic resonance imaging study. Parkinsonism & related disorders. 2016; 25:78–84. [PubMed: 26876036]

[11]. Lehericy S, Tijssen MA, Vidailhet M, Kaji R, Meunier S. The anatomical basis of dystonia: current view using neuroimaging. Mov Disord. 2013; 28:944–957. [PubMed: 23893451]

[12]. Fuertinger S, Horwitz B, Simonyan K. The Functional Connectome of Speech Control. PLoS Biol. 2015; 13:e1002209. [PubMed: 26204475]

[13]. Simonyan K, Berman BD, Herscovitch P, Hallett M. Abnormal striatal dopaminergic neurotransmission during rest and task production in spasmodic dysphonia. J Neurosci. 2013; 33:14705–14714. [PubMed: 24027271]

[14]. Biswal B, Yetkin FZ, Haughton VM, Hyde JS. Functional connectivity in the motor cortex of resting human brain using echo-planar MRI. Magn Reson Med. 1995; 34:537–541. [PubMed: 8524021]

[15]. Damoiseaux JS, Greicius MD. Greater than the sum of its parts: a review of studies combining structural connectivity and resting-state functional connectivity. Brain Struct Funct. 2009; 213:525–533. [PubMed: 19565262]

[16]. Smith SM, Fox PT, Miller KL, et al. Correspondence of the brain's functional architecture during activation and rest. Proc Natl Acad Sci U S A. 2009; 106:13040–13045. [PubMed: 19620724]

[17]. Dresel C, Li Y, Wilzeck V, Castrop F, Zimmer C, Haslinger B. Multiple changes of functional connectivity between sensorimotor areas in focal hand dystonia. J Neurol Neurosurg Psychiatry. 2014; 85:1245–1252. [PubMed: 24706945]

[18]. Delnooz CC, Pasman JW, Beckmann CF, van de Warrenburg BP. Altered striatal and pallidal connectivity in cervical dystonia. Brain Struct Funct. 2015; 220:513–523. [PubMed: 24259114]

[19]. Zhou B, Wang J, Huang Y, Yang Y, Gong Q, Zhou D. A resting state functional magnetic resonance imaging study of patients with benign essential blepharospasm. J Neuroophthalmol. 2013; 33:235–240. [PubMed: 23636105]

[20]. Mohammadi B, Kollewe K, Samii A, Beckmann CF, Dengler R, Munte TF. Changes in resting-state brain networks in writer's cramp. Hum Brain Mapp. 2012; 33:840–848. [PubMed: 21484954]

[21]. Termsarasab P, Ramdhani RA, Battistella G, et al. Neural correlates of abnormal sensory discrimination in laryngeal dystonia. NeuroImage: Clinical. 2015

[22]. Fornari E, Maeder P, Meuli R, Ghika J, Knyazeva MG. Demyelination of superficial white matter in early Alzheimer's disease: a magnetization transfer imaging study. Neurobiol Aging. 2012; 33:428. e427-419.

[23]. Janousova E, Schwarz D, Kasparek T. Combining various types of classifiers and features extracted from magnetic resonance imaging data in schizophrenia recognition. Psychiatry Res. 2015; 232:237–249. [PubMed: 25912090]

[24]. Yourganov G, Schmah T, Churchill NW, Berman MG, Grady CL, Strother SC. Pattern classification of fMRI data: applications for analysis of spatially distributed cortical networks. Neuroimage. 2014; 96:117–132. [PubMed: 24705202]

[25]. Yun HJ, Kwak K, Lee JM, Alzheimer's Disease Neuroimaging I. Multimodal Discrimination of Alzheimer's Disease Based on Regional Cortical Atrophy and Hypometabolism. PLoS One. 2015; 10:e0129250. [PubMed: 26061669]

[26]. Zhang D, Liu X, Chen J, Liu B. Distinguishing patients with Parkinson's disease subtypes from normal controls based on functional network regional efficiencies. PLoS One. 2014; 9:e115131. [PubMed: 25531436]

[27]. Bauer AJ, Just MA. Monitoring the growth of the neural representations of new animal concepts. Hum Brain Mapp. 2015; 36:3213–3226. [PubMed: 26032608]

[28]. Just MA, Cherkassky VL, Buchweitz A, Keller TA, Mitchell TM. Identifying autism from neural representations of social interactions: neurocognitive markers of autism. PLoS One. 2014; 9:e113879. [PubMed: 25461818]

[29]. Mason RA, Just MA. Physics instruction induces changes in neural knowledge representation during successive stages of learning. Neuroimage. 2015; 111:36–48. [PubMed: 25665967]

[30]. Hale JR, Mayhew SD, Mullinger KJ, et al. Comparison of functional thalamic segmentation from seed-based analysis and ICA. Neuroimage. 2015; 114:448–465. [PubMed: 25896929]

[31]. Leech R, Kamourieh S, Beckmann CF, Sharp DJ. Fractionating the default mode network: distinct contributions of the ventral and dorsal posterior cingulate cortex to cognitive control. J Neurosci. 2011; 31:3217–3224. [PubMed: 21368033]

[32]. Sami S, Robertson EM, Miall RC. The time course of task-specific memory consolidation effects in resting state networks. J Neurosci. 2014; 34:3982–3992. [PubMed: 24623776]

[33]. Smith DV, Utevsky AV, Bland AR, et al. Characterizing individual differences in functional connectivity using dual-regression and seed-based approaches. Neuroimage. 2014; 95:1–12. [PubMed: 24662574]

[34]. Kaufmann T, Skatun KC, Alnaes D, et al. Disintegration of Sensorimotor Brain Networks in Schizophrenia. Schizophr Bull. 2015

[35]. Nugent AC, Robinson SE, Coppola R, Furey ML, Zarate CA Jr. Group differences in MEG-ICA derived resting state networks: Application to major depressive disorder. Neuroimage. 2015; 118:1–12. [PubMed: 26032890]

[36]. Argyelan M, Gallego JA, Robinson DG, et al. Abnormal resting state FMRI activity predicts processing speed deficits in first-episode psychosis. Neuropsychopharmacology. 2015; 40:1631–1639. [PubMed: 25567423]

[37]. Tinaz S, Lauro P, Hallett M, Horovitz SG. Deficits in task-set maintenance and execution networks in Parkinson's disease. Brain Struct Funct. 2015

[38]. Ashburner J, Friston KJ. Unified segmentation. Neuroimage. 2005; 26:839–851. [PubMed: 15955494]

[39]. Bishop, CM. Pattern recognition and machine learning. Springer; New York: 2006.

[40]. Beckmann CF, Smith SM. Probabilistic independent component analysis for functional magnetic resonance imaging. IEEE transactions on medical imaging. 2004; 23:137–152. [PubMed: 14964560]

[41]. van den Heuvel MP, Hulshoff Pol HE. Exploring the brain network: a review on resting-state fMRI functional connectivity. Eur Neuropsychopharmacol. 2010; 20:519–534. [PubMed: 20471808]

[42]. Delnooz CC, Helmich RC, Toni I, van de Warrenburg BP. Reduced parietal connectivity with a premotor writing area in writer's cramp. Mov Disord. 2012; 27:1425–1431. [PubMed: 22886735]

[43]. Hinkley LB, Sekihara K, Owen JP, Westlake KP, Byl NN, Nagarajan SS. Complex-value coherence mapping reveals novel abnormal resting-state functional connectivity networks in task-specific focal hand dystonia. Front Neurol. 2013; 4:149. [PubMed: 24133480]

[44]. Filippini N, MacIntosh BJ, Hough MG, et al. Distinct patterns of brain activity in young carriers of the APOE-epsilon4 allele. Proc Natl Acad Sci U S A. 2009; 106:7209–7214. [PubMed: 19357304]

[45]. Beckmann CF, DeLuca M, Devlin JT, Smith SM. Investigations into resting-state connectivity using independent component analysis. Philos Trans R Soc Lond B Biol Sci. 2005; 360:1001–1013. [PubMed: 16087444]

[46]. Berardelli A, Rothwell JC, Day BL, Marsden CD. Pathophysiology of blepharospasm and oromandibular dystonia. Brain. 1985; 108:593–608. Pt 3. [PubMed: 4041776]

[47]. Marsden CD. Motor disorders in basal ganglia disease. Hum Neurobiol. 1984; 2:245–250. [PubMed: 6715209]

[48]. Burton K, Farrell K, Li D, Calne DB. Lesions of the putamen and dystonia: CT and magnetic resonance imaging. Neurology. 1984; 34:962–965. [PubMed: 6539874]

[49]. Simonyan K, Fuertinger S. Speech networks at rest and in action: interactions between functional brain networks controlling speech production. J Neurophysiol. 2015; 113:2967–2978. [PubMed: 25673742]

[50]. Hickok G, Poeppel D. The cortical organization of speech processing. Nat Rev Neurosci. 2007; 8:393–402. [PubMed: 17431404]

[51]. Samargia S, Schmidt R, Kimberley TJ. Shortened cortical silent period in adductor spasmodic dysphonia: evidence for widespread cortical excitability. Neurosci Lett. 2014; 560:12–15. [PubMed: 24333913]

[52]. Samargia S, Schmidt R, Kimberley TJ. Cortical Silent Period Reveals Differences Between Adductor Spasmodic Dysphonia and Muscle Tension Dysphonia. Neurorehabil Neural Repair. 2016; 30:221–232. [PubMed: 26089309]

[53]. Neychev VK, Gross RE, Lehericy S, Hess EJ, Jinnah HA. The functional neuroanatomy of dystonia. Neurobiol Dis. 2011; 42:185–201. [PubMed: 21303695]

[54]. Zoons E, Booij J, Nederveen AJ, Dijk JM, Tijssen MA. Structural, functional and molecular imaging of the brain in primary focal dystonia--a review. Neuroimage. 2011; 56:1011–1020. [PubMed: 21349339]

[55]. Bielamowicz S, Ludlow CL. Effects of botulinum toxin on pathophysiology in spasmodic dysphonia. Ann Otol Rhinol Laryngol. 2000; 109:194–203. [PubMed: 10685573]

[56]. Brownsett SL, Wise RJ. The contribution of the parietal lobes to speaking and writing. Cereb Cortex. 2010; 20:517–523. [PubMed: 19531538]

[57]. Culham JC, Valyear KF. Human parietal cortex in action. Curr Opin Neurobiol. 2006; 16:205–212. [PubMed: 16563735]

[58]. Shum M, Shiller DM, Baum SR, Gracco VL. Sensorimotor integration for speech motor learning involves the inferior parietal cortex. Eur J Neurosci. 2011; 34:1817–1822. [PubMed: 22098364]

[59]. Sereno MI, Huang RS. Multisensory maps in parietal cortex. Curr Opin Neurobiol. 2014; 24:39–46. [PubMed: 24492077]

[60]. Gottlieb J. From thought to action: the parietal cortex as a bridge between perception, action, and cognition. Neuron. 2007; 53:9–16. [PubMed: 17196526]

[61]. de Vries PM, Johnson KA, de Jong BM, et al. Changed patterns of cerebral activation related to clinically normal hand movement in cervical dystonia. Clin Neurol Neurosurg. 2008; 110:120–128. [PubMed: 18006221]

[62]. Fiorio M, Weise D, Onal-Hartmann C, Zeller D, Tinazzi M, Classen J. Impairment of the rubber hand illusion in focal hand dystonia. Brain. 2011; 134:1428–1437. [PubMed: 21378099]

[63]. Hagura N, Oouchida Y, Aramaki Y, et al. Visuokinesthetic perception of hand movement is mediated by cerebro-cerebellar interaction between the left cerebellum and right parietal cortex. Cereb Cortex. 2009; 19:176–186. [PubMed: 18453537]

[64]. Fuchs T, Saunders-Pullman R, Masuho I, et al. Mutations in GNAL cause primary torsion dystonia. Nature genetics. 2013; 45:88–92. [PubMed: 23222958]

[65]. Ozelius LJ, Lubarr N, Bressman SB. Milestones in dystonia. Mov Disord. 2011; 26:1106–1126. [PubMed: 21626555]

[66]. Parker N. Hereditary whispering dysphonia. J Neurol Neurosurg Psychiatry. 1985; 48:218–224. [PubMed: 3156966]

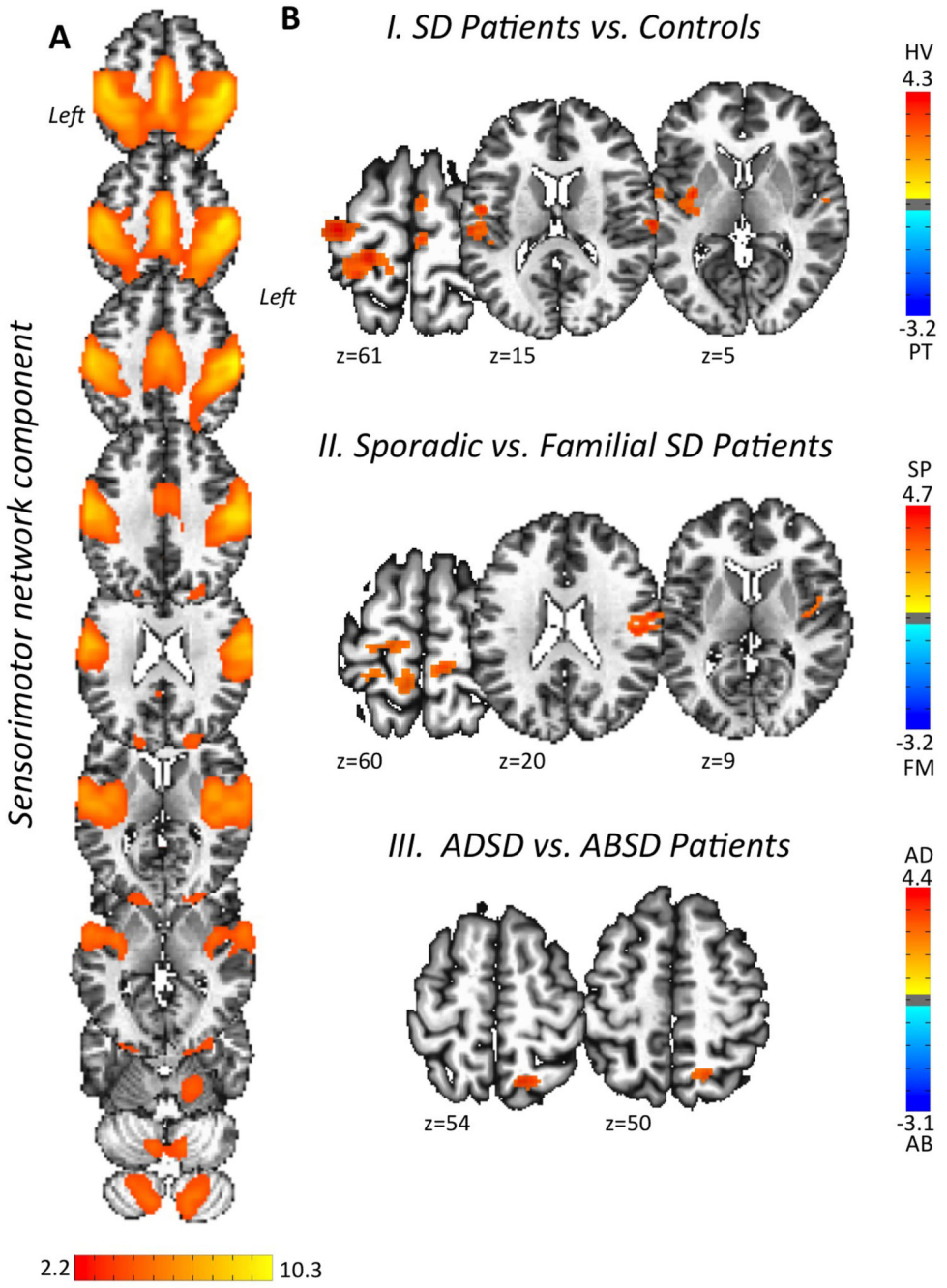

Figure 1. Sensorimotor functional network alteration assessed using independent component analysis (ICA)

Panel (A) shows the sensorimotor network extracted across all SD patients and controls. Voxel-based inferential statistics were used to compare (B-I) all SD patients vs. healthy controls, (B-II) sporadic vs. familial SD patients, and (B-III) ADSD vs. ABSD patients. Statistical maps are superimposed on a series of axial slices of the standard brain in Talairach-Tournoux space. The color bars represent Z scores for independent components and t scores for group statistical comparisons ($p \leq 0.01$, FWE-corrected). AB – abductor SD

patients; AD – adductor SD patients; FM – familial SD patients; HV – healthy control volunteers; PT – patients; SD – spasmodic dysphonia; SP – sporadic SD patients.

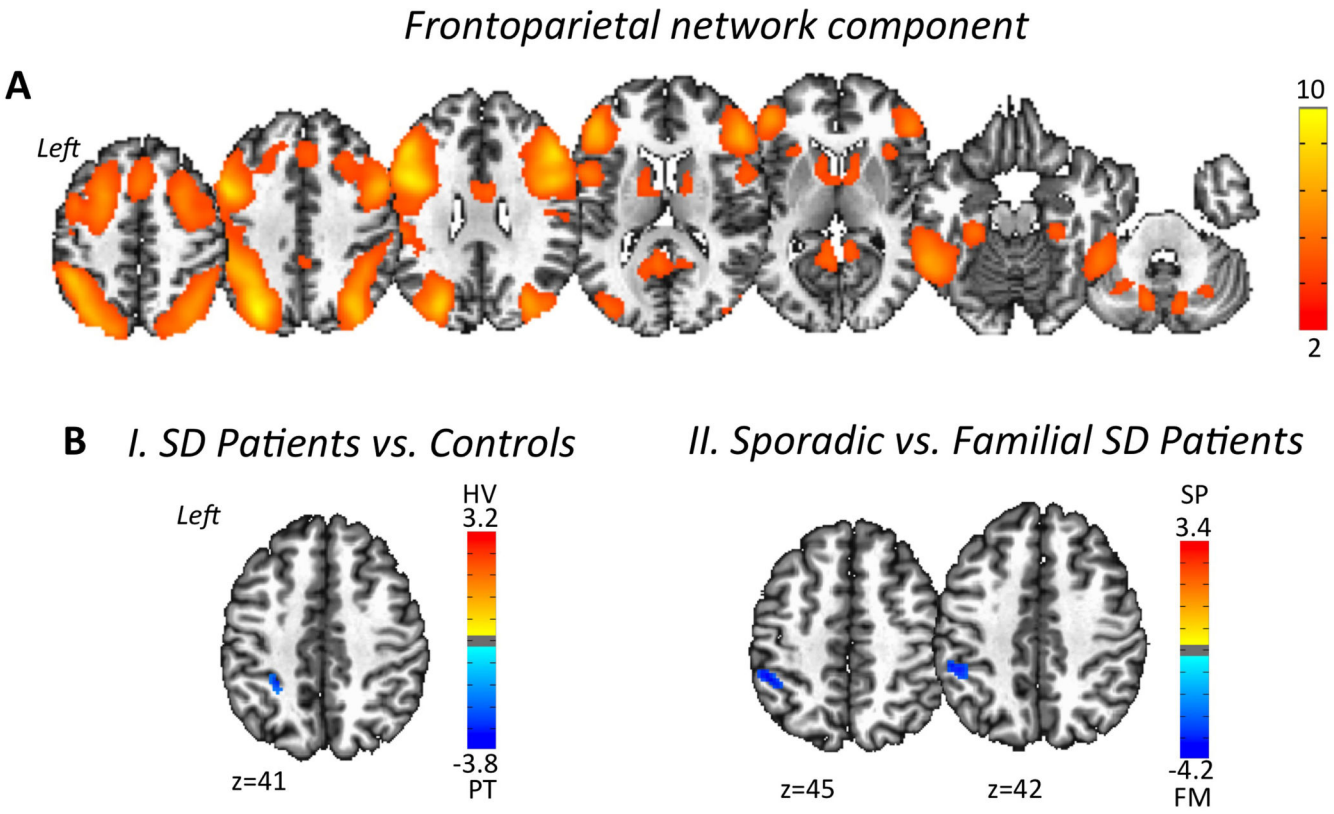

Figure 2. Frontoparietal functional network alteration assessed using independent component analysis (ICA)

Panel (A) shows the frontoparietal network extracted across all SD patients and controls. Voxel-based inferential statistics were used to compare (B-I) all SD patients vs. healthy volunteers, and (B-II) sporadic vs. familial SD patients. Statistical maps are superimposed on a series of axial slices of the standard brain in Talairach-Tournoux space. The color bars represent Z scores for independent components and t scores for group statistical comparisons ($p \leq 0.01$, FWE-corrected). FM – familial SD patients; HV – healthy control volunteers; PT – patients; SD – spasmodic dysphonia; SP – sporadic SD patients.

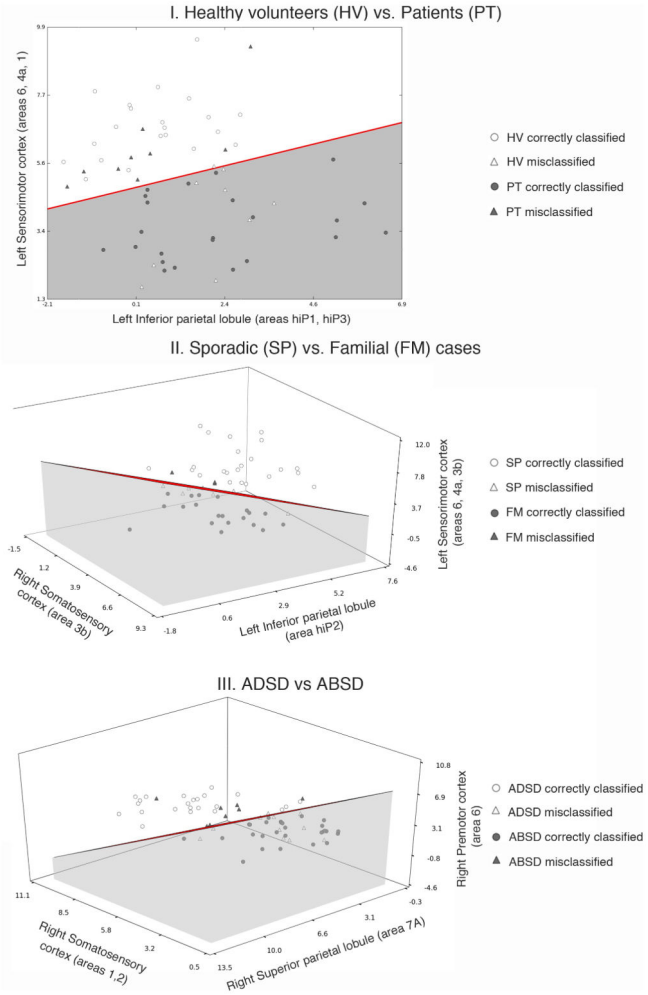

Figure 3. Results of the linear discriminant analysis of (I) SD patients vs healthy volunteers, (II) sporadic vs familial SD patients, and (III) ADSD vs ABSD patients

The scatter plots show the individual combinations of the mean values of the *Z* score within (I) the left sensorimotor and the left inferior parietal cortices in patients (gray circles for correct classification and gray triangles for misclassification of patients) and healthy volunteers (empty circles for correct classification and empty triangles for misclassified helthy volunteers); (II) the left inferior parietal lobule, right somatosensory, and left sensorimotor cortices in sporadic SD (empty circles for correct classification and empty triangles for misclassification of sporadic patients) and familial SD (gray circles for correct classification and gray triangles for misclassification of familial patients); (III) the right superior parietal lobule, somatosensory and premotor cortices in ABSD (gray circles for correct classification and gray triangles for ABSD patients misclassified) and ADSD (empty circles for correct classification and empty triangles for misclassified ADSD) patients. The red line (I) and red planes (II and III) represent the decision boundary of the classification. The corresponding values are provided in Table 3. AB – abductor SD patients; AD – adductor SD patients; FM – familial SD patients; HV – healthy control volunteers; PT – patients; SP – sporadic SD patients.

Table 1

Demographic characteristics and clinical data

	Sporadic		Familial		Controls
	ADSD	**ABSD**	**ADSD**	**ABSD**	
Number of subjects	30	30	18	5	30
Age (years; mean± standard deviation)	55.4±8.3	52.9±12.7	56.3±15.5	63.4±5.8	49.7±9.5
Gender (Female/Male)	23/7	26/4	16/2	2/3	18/12
Ethnicity (Caucasian/African-American/Other	28/1/1	26/3/1	16/0/0	5/0/0	16/11/3
Handedness (Edinburgh Inventory)	Right				
Language	Monolingual native English				
Cognitive status	Mini-Mental State Examination ≥ 27 points				
Genetic status	Negative for DYT1, DYT6, DYT4 and DYT25				
Disease Duration (years; mean ± standard deviation)	11.8±9	15±9.3	19.7±13.9	19.2±13.4	N/A
Age of onset (mean ± standard deviation)	43.6±11.2	38±12.7	36.6±16.7	44.2±12.9	N/A

Table 2

Peaks of activation of the significant clusters showing differences between the groups in the sensorimotor and frontoparietal network components

Sensorimotor Network Component				
Brain cluster	*Talairach coordinates at a cluster peak (x, y, z)*			*t-score*
Patients vs. Controls				
L Sensorimotor cortex (areas 6, 4a, 1)	−22	−32	63	4.27
L Supramarginal gyrus (area PFop)	−60	−26	23	4.3
L Putamen	−30	−6	7	4.1
R Supplementary motor area	2	−4	57	4.2
R Parietal operculum/Primary auditory cortex (area OP1/TE 1.0)	62	−18	15	3.7
Sporadic vs. Familial SD				
L Sensorimotor cortex (areas 6, 4a, 3b)	−18	−22	65	4.7
R Primary somatosensory cortex (area 3b)	58	−6	21	4.1
R Supplementary motor area	6	−30	49	3.9
ADSD vs. ABSD				
R Superior parietal lobule (area 7A)	12	−60	53	3.8
R Primary somatosensory cortex (areas 1, 2)	48	−34	51	2.94
R Premotor cortex (area 6)	50	−10	49	3.29
Frontoparietal Network Component				
Patients vs. Controls				
L Inferior parietal lobule (areas hIP1, hIP3)	−26	−42	37	3.8
Sporadic vs. Familial SD				
L Inferior parietal lobule (hlP2)	−46	−40	43	4.2

Table 3

Performance of the linear discriminant analysis (LDA)

SD Patients vs. Healthy Controls			
Brain region	*Accuracy rate*	*Misclassification rate*	
		SD Patients	*Healthy Controls*
L Inferior Parietal Lobule	50%	53% (17/32)	47% (14/30)
L Inferior Parietal Lobule & L Sensorimotor Cortex	71%	28% (9/32)	30% (9/30)
Familial SD vs. Sporadic SD			
Brain region	*Accuracy rate*	*Misclassification rate*	
		Familial SD	*Sporadic SD*
L Inferior Parietal Lobule	68%	35% (8/23)	39% (9/30)
L Inferior Parietal Lobule & R Sensorimotor Cortex & L Premotor Cortex	81%	13% (3/23)	23% (7/30)
ADSD vs. ABSD			
Brain region	*Accuracy rate*	*Misclassification rate*	
		ADSD	*ABSD*
R Superior Parietal Lobule	65%	37% (13/35)	31% (11/35)
R Superior Parietal Lobule & R Primary Somatosensory Cortex & R Premotor Cortex	71%	34% (12/35)	23% (8/35)